# Mismatched dynamics of dissolved organic carbon and chromophoric dissolved organic matter in the coastal NW Mediterranean Sea

Elvia D.Sánchez-Pérez, Mireille Pujo-Pay, Eva Ortega-Retuerta, Pascal Conan, Francesc Peters, Cèlia Marrasé

# Mismatched dynamics of dissolved organic carbon and chromophoric dissolved organic matter in the coastal NW Mediterranean Sea

Elvia D. Sánchez-Pérez [a,c,*,1], Mireille Pujo-Pay [b], Eva Ortega-Retuerta [b], Pascal Conan [c], Francesc Peters [a], Cèlia Marrasé [a]

[a] ICM-CSIC, Institut de Ciències del Mar, Passeig Marítim de la Barceloneta 37-49, 08003 Barcelona, Catalunya, Spain
[b] CNRS, UMR 7621, Laboratoire d'Océanographie Microbienne, Observatoire Océanologique, F-666650 Banyuls/mer, France
[c] Sorbonne Université, UMR 7621, Laboratoire d'Océanographie Microbienne, Observatoire Océanologique, F-66650 Banyuls/mer, France

## HIGHLIGHTS

- DOM composition monitored during 15 months in a NW Mediterranean coastal station.
- Fluorescent DOM dynamics was influenced by freshwater intrusions.
- A decrease in nutrients due to stratification promoted surface DOC accumulation.
- A temporal mismatch was found between chlorophyll *a* and dissolved organic matter.

## GRAPHICAL ABSTRACT
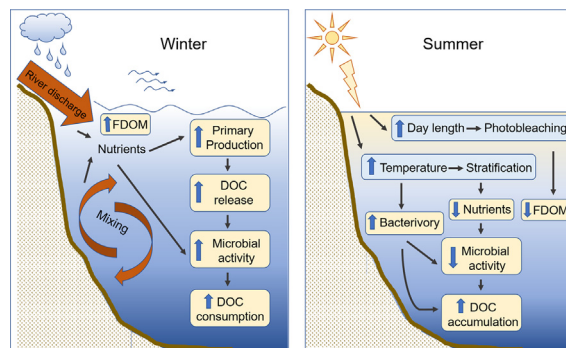


## ARTICLE INFO

## ABSTRACT

Coastal marine ecosystems are strongly influenced by different occasional events, such as intense winds, mixing, rain and river discharges. These events can directly or indirectly cause changes in dissolved organic matter (DOM) quality through a cascade of different biotic and abiotic processes. Changes in DOM quality are often associated with changes in DOM optical properties. Thus, examining the dynamics of chromophoric DOM (CDOM) can provide valuable information about biological and physical processes that have occurred in the ecosystem. Episodic meteorological events, particularly in temperate areas, appear very abruptly and induce very rapid responses; therefore, high time-resolved measurements are needed to capture them. We used a weekly sampling scheme to characterize DOM and nutrient dynamics in the NW Mediterranean coastal station 'SOLA'. From February 2013 to April 2014, we measured several physical and chemical variables including temperature, salinity, inorganic nutrients, chlorophyll *a* dissolved organic carbon (DOC), CDOM and fluorescent DOM (FDOM). During this period, two extremely high fresh water intrusions greatly influenced the dynamics of some DOM fractions, in particular the FDOM. Inorganic nutrients and chlorophyll *a* showed seasonal patterns: A winter period characterized by a high nutrient concentration in surface waters favored the phytoplankton spring bloom; then, summer stratification extended until autumn. This stratification led to nutrient depletion and, consequently, lower chlorophyll *a* values in the photic zone. The CDOM and FDOM optical active fractions did not follow temporal trends similar to total DOC. This was likely because the potential sources and sinks of these DOM pools are microbial activity

---

* Corresponding author at: Sorbonne Université, UMR 7621, Laboratoire d'Océanographie Microbienne, Observatoire Océanologique, F-66650 Banyuls/mer, France.
*E-mail address:* celia@icm.csic.es (E.D. Sánchez-Pérez).
1 CONACyT-Instituto Politécnico Nacional-Centro Interdisciplinario de Ciencias Marinas (IPN-CICIMAR), Departamento de Plancton y Ecología Marina, La Paz, BCS, México.

and light exposure, and these were acting simultaneously but in opposite directions. Interestingly, DOC exhibited the highest concentrations in summer, coinciding with nutrient and chlorophyll *a* minima. To explain this mismatch, we propose a sequence of abiotic and biotic phenomena that drive DOC temporal dynamics.

## 1. Introduction

With 660 Pg C, the oceanic dissolved organic matter (DOM) pool represents one of Earth's largest organic carbon reservoirs, an amount equivalent to C as atmospheric $CO_2$ (Hedges, 2002). Therefore, the mechanisms that produce and recycle DOM in the ocean are crucial for predicting further changes in $CO_2$ captured by the ocean (Wagner et al., 2020). Chromophoric Dissolved Organic Matter (CDOM) is the fraction of dissolved organic matter comprised by optically active compounds. CDOM in oceanic regions represents about 70% of the total dissolved organic carbon (DOC), and this percentage can increase in areas with a riverine influence (Blough and Del Vecchio, 2002; Coble, 2007). Given that light absorption by CDOM occurs mainly in the ultraviolet spectra, this DOM pool is key in regulating UV light penetration in the water column and its consequent damages to biological communities (Kuwahara et al., 2000). However, its significant absorption also in the visible spectra interferes with primary production. This last effect is particularly remarkable in view of efforts to estimate chlorophyll *a* concentration from space (Böhm et al., 2016). In addition, CDOM measurements allow us to calculate indexes that provide information about chemical structure and biogeochemical processes of DOM in aquatic environments (Green and Blough, 1994). For example, the specific absorption coefficient at 254 nm [$a$*CDOM(254)], has been used as a proxy for aromaticity (Weishaar et al., 2013), and the slope of the CDOM absorption spectrum can be used as a surrogate of DOM molecular weight (Helms et al., 2008)

The CDOM fraction which contains compounds that emit light when excited by ultraviolet radiation is called fluorescent dissolved organic matter (FDOM). FDOM dynamics in aquatic systems have been characterized using fluorescence spectroscopy analyses and, in particular, measurements of Excitation-Emission Matrices (EEMs) (Blough and Del Vecchio, 2002; Nieto-Cid et al., 2006; Romera-Castillo et al., 2010). Coble (1996) used EEMs to define different groups of substances that provide complementary information about DOM origin and lability. In the present study, we focus on two humic-like types (peak–M, and peak–C) and one protein-like type (peak–T). Peak–M has been related to marine prokaryotic heterotrophic activity (Coble et al., 1998; Romera-Castillo et al., 2011a), while peak–C substances are mostly associated with materials of terrestrial origin (Coble, 1996; Nieto-Cid et al., 2006). However, some field and experimental studies have shown that peak–C can also be produced by marine microorganisms (Romera-Castillo et al., 2011b; De La Fuente et al., 2014). Humic-like substances are considered to be recalcitrant but exhibit high photolability, in contrast to protein-like peak–T compounds that are considered as a tracer for biologically labile DOM (Yamashita and Tanoue, 2003). Therefore, the protein-like vs humic-like ratio (peak-T/peak-C) has been used as a proxy of DOM lability.

CDOM and FDOM in Mediterranean coastal areas exhibit contrasting temporal patterns depending on the particular site and year (Para et al., 2010; Romera-Castillo et al., 2013). In these coastal systems, plankton dynamics are also highly variable (Cloern and Jassby, 2008; Romero et al., 2014). This high variability emerges from the complex responses of the systems to both seasonal and episodic meteorological events. However, previous sampling efforts in the area have not been intensive enough to capture the response to these episodic phenomena. Here, in order to capture the signal of both types of variability sources and their direct or indirect influence on DOM dynamics, we sampled a coastal station located in the NW Mediterranean on a weekly basis during 14-months (SOLA Station, Banyuls sur Mer, France). The aim of our work was to determine the major environmental drivers affecting the dissolved organic matter (DOM) concentration and quality in this area with the aim of discerning recurrent seasonal dynamics from episodic phenomena. To achieve this, we first analyzed samples for different DOM fractions together with several environmental variables during a 14-month period. Then, we compared our results with climatological and environmental data (temperature, salinity and inorganic nutrient and chlorophyll *a* concentrations) collected from January 2000 to April 2014 at the same station.

## 2. Material and methods

### 2.1. Site and sample collection

Samples were taken from a NW Mediterranean coastal station (station SOLA, 42°30′ N, 03°09′ E, 27 m depth), located in the Bay of Banyuls sur Mer. The area receives the discharge of two rivers, the Têch and Têt Rivers. The mouths of the rivers are located at approximately 14 and 27 km north (Fig. 1) and the area is influenced by winter windstorms. Samples for nutrients, chlorophyll *a* and DOM analyses were collected directly from Niskin bottles weekly at 3 m depth from February 2013 to April 2014 aboard the RV "Nereis II". We also compiled results from the SOLA station database to examine the temporal trends of a 14-year period (2000–2014).

Temperature and salinity were simultaneously measured using a Seabird 19 Conductivity-Temperature-Depth probe. The data analyzed from the historical time series (years 2000 to 2012) were acquired
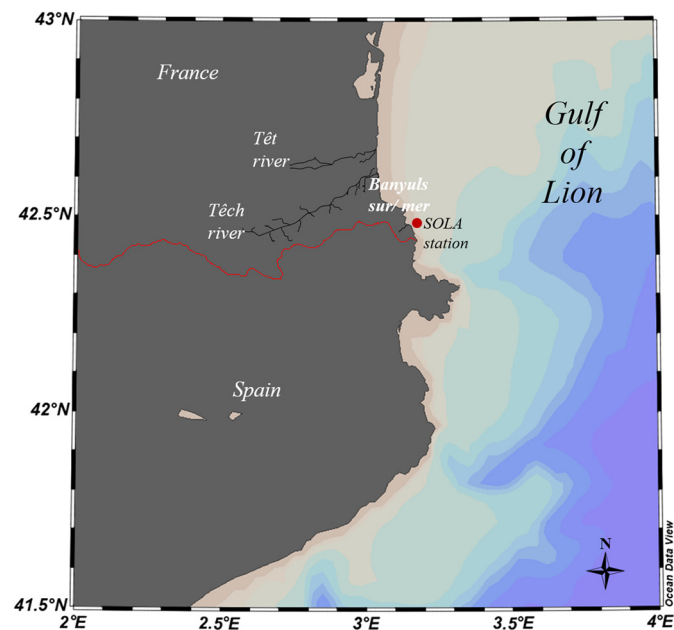


**Fig. 1.** Map of the study area. The red circle represents the SOLA station. The black lines represent the Têch and Têt Rivers.

from the French Coastline Observation Service (http://somlit.epoc.u-bordeaux1.fr/fr).

Discharge data of the Têt and Têch Rivers for the period 2010–2014 were obtained from the hydro database (http://www.hydro.eaufrance.fr/).

## 2.2. Chemical and biological analyses

Chlorophyll *a* concentration was determined by fluorimetry. For each sample, 250 mL of seawater was filtered on a Whatman GF/F 25 mm glass fiber filter. All filters were stored at −20 °C until analysis. After extraction by 90% acetone during 24 h in the dark; the total chlorophyll and phaeopigment concentrations were measured using a Tuner Design 10-AU fluorimeter (Holm-Hansen et al., 1965) calibrated with standard solid RD-AU10. Samples for inorganic nutrient analyses ($NO_3^-$, $PO_4^{-3}$ and $H_4SiO_4$) were collected in 12 mL polyethylene tubes and stored at −20 °C until analysis in the laboratory using a colorimetric "Seal-Bran-Luebb AA3HR" auto-analyzer (Germany). Dissolved $NH_4^+$ concentrations were determined in fresh samples using a nanomolar fluorometric method according to Holmes et al. (1999) on a fluorometer Jasco FP-2020. The accuracy of the measurements was ±0.02 μmol L$^{-1}$ for nitrate ($NO_3^-$), ±0.05 μmol L$^{-1}$ for silicate ($H_4SiO_4$), ±0.01 μmol L$^{-1}$ for phosphate ($PO_4^{-3}$) and ± 2 nM for ammonium ($NH_4^+$).

Samples for dissolved organic carbon (DOC) analyses were filtered through pre-combusted Whatman GF/F filters (nominal pore size 0.7 μm) and collected in pre-combusted (12 h at 450 °C) glass ampoules. After acidification with orthophosphoric acid ($H_3PO_4$ _50 μL) to pH < 2, the ampoules were heat sealed and stored in the dark until analysis. DOC was analyzed following the high temperature catalytic oxidation (HTCO) technique (Sugimura and Suzuki, 1998; Cauwet, 1999) using a Shimadzu TOC-L analyzer. The system was calibrated daily with a solution of acetanilide ($C_8H_9NO$ MW = 135.17).

For particulate organic carbon (POC) analyses, 1 L seawater samples were filtered on pre-combusted (24 h, 450 °C) glass fiber filters (Whatman GF/F, 25 mm). The filters were dried overnight at 50 °C and stored in glass vials in a desiccator until analyzed according to the wet oxidation method described by Pujo-Pay and Raimbault (1994) using a CHN Perking Elmer 2400.

## 2.3. Chromophoric (CDOM) and fluorescent (FDOM) dissolved organic matter analyses

Samples for DOM absorption (CDOM) and fluorescence (FDOM) were filtered by gravity through 47 mm pre-combusted Whatman GF/F filters (nominal pore size 0.7 μm) into 250 mL pre-combusted (24 h at 450 °C) glass flasks. We chose GF/F filters instead of 0.2 μm pore size filters for our filtrations because GF/F filters have been and are extensively used for oceanographic and biogeochemical analyses. Moreover, they can be combusted at high temperatures, which minimizes contamination. Actually, as they shrink slightly after combustion they are comparable to 0.2 μm filters in oligotrophic waters. A previous study (Ferrari, 2000) found no significant differences in CDOM measurements when it compared samples filtered through GF/F and 0.2 μm pore size filters in Western Mediterranean waters. The filtered samples were subsequently frozen at −20 °C in the dark until analysis in the laboratory. Although freezing can alter the structure of some DOM compounds, recent studies have reported minimal changes in DOM due to storage (Hancke et al., 2014). However, to evaluate these effects, a test was carried out with coastal water DOM samples from the Blanes Bay Microbial Observatory, NW Mediterranean (BBMO, 41°40′0″ N, 2°48′0″ E). FDOM was measured ($n = 8$) in fresh and in thawed samples after being frozen at −20 °C for eight months. We found no significant differences between the fresh and frozen samples in any FDOM peaks (*t*-test, $p > 0.05$). CDOM absorbance was measured in 10 cm quartz cuvettes using a Varian Cary UV-VIS spectrophotometer. Absorbance spectra were performed between 250 and 750 nm at a constant room temperature of 20 °C, with Milli-Q water as reference blank. The

residual backscattering (colloidal material, fine size particle fractions present in the sample) was corrected by subtracting the mean absorbance from 600 to 750 nm (Bricaud et al., 1981). The CDOM absorption coefficient ($a_\lambda$) in m$^{-1}$ at λ was calculated according to Eq. (1):

$$a_{(\lambda)} = Abs_{(\lambda)} * 2303/l \tag{1}$$

where $Abs_{(\lambda)}$ is the absorbance at λ wavelength, *l* is the optical path length (m) and 2.303 is a factor for the conversion of the Decimal logarithm to the Napierian logarithm. CDOM spectral slopes were calculated over the wavelength ranges 250–500 nm and 275–295 nm using linear regressions of the natural log-transformed $a_{CDOM}$ (λ) according to Nelson et al. (2004) and Helms et al. (2008).

FDOM samples were analyzed with a Perkin Elmer luminescence spectrometer LS 55 (United Kingdom) equipped with a xenon discharge lamp, equivalent to 20 kW. Slit widths were 10.0 nm for the wavelengths of excitation and emission and the scan speed was 250 nm min$^{-1}$.

Matrices (EEMs) were generated by combining 21 synchronous excitation-emission fluorescence spectra of the sample, obtained for an excitation wavelength range of 250–450 nm and a 20 nm offset between the excitation and emission wavelengths. The instrument was calibrated with a quinine sulfate dehydrate (QS) standard made up in 0.05 mol L$^{-1}$ of sulfuric acid (Nieto-Cid et al., 2006). Therefore, fluorescence measurements were expressed in quinine sulfate units (QSU). Milli-Q water was used as a blank and Raman scattering was corrected by subtracting the EEM of the Milli-Q water from the EEM of the samples. Inner Filter Effect (IFE) corrections were not applied to fluorescence measurements. According to previous studies (Ohno, 2002, Stedmon and Bro, 2008, Kothawala et al., 2013, Wang et al., 2017), the inner filter effects on fluorescence measurements are negligible (<5%) when absorbance values are lower than 0.04 (absorption coefficient below 10 m$^{-1}$) and thus IFE corrections are not necessary. In our data series, the absorbance values ranged from 0.005 to 0.02. Within this range of absorbances, the percent measurement error for non-corrected FDOM values would range from 1.12 to 1.21%. We used a combination of different pairs of excitation-emission (EX/EM) wavelengths previously described by Coble (1996) in order to compare our results with previous studies.

The fluorescence quantum yield at 340 nm was determined using the ratio of the absorption coefficient at 340 nm and the corresponding fluorescence emission between 400 and 600 nm of the water sample and referred to the QS standard ratio (Green and Blough, 1994) according to Eq. (2):

$$\Phi(340) = \frac{F(400-600)}{a_{CDOM}(340)} \cdot \frac{a_{CDOM}(340)_{QS}}{F(400-600)_{QS}} \cdot \Phi(340)_{QS} \tag{2}$$

where $a_{CDOM}(340)$ and $a_{CDOM}(340)_{QS}$ are the absorption coefficients of the sample and of the QS standard, respectively at 340 nm (in m$^{-1}$); $F(400–600)$ and $F(400–600)_{QS}$ are the average integrated fluorescence spectra between 400 and 600 nm at a fixed excitation wavelength of 340 nm obtained for each sample and for the QS standard (Romera-Castillo et al., 2011a); $\Phi(340)_{QS}$ is the dimensionless fluorescence quantum yield of the QS standard and equals 0.54 (Melhuish, 1961). The specific absorption coefficient $a^*_{CDOM}$ (254) was obtained by dividing the value $a_{CDOM}$ (254) by the DOC concentration and was expressed in m$^2$ g C$^{-1}$.

## 2.4. Statistical analyses

Pearson correlations were determined to explore co-occurrence patterns between DOM metrics and environmental parameters. Data were log10-transformed to accomplish the requirements of parametric tests. Data normality was tested using Kolmogorov-Smirnov tests. A correlation matrix was generated to explore the

co-occurrence patterns between physical and chemical properties at our sampling site. A multiple regression was applied to autumn-winter samples to explore the FDOM variability as a function of salinity and Chl a.

# 3. Results

## 3.1. Hydrological and physiochemical parameters – Long term period (2000–2014)

The long-term temporal dynamics of the measured variables showed a strong seasonal signal during the time series. In this section, we describe seasonal variability of averaged values over the study years (see Figs. 2). The discharges of both the Têch and Têt Rivers showed three well-defined periods: the spring period with high flow (March to May, mean 11.5 ± 11.6 and 13.1 ± 13.7 m$^3$s$^{-1}$ respectively), followed by a low flow scenario during mid-summer and early autumn (July to September, mean 1.61 ± 1.16 and 2.8 ± 2.1 m$^3$s$^{-1}$ respectively) and continuing with an interval of moderate flow from mid-autumn to early winter (October to December, mean 7.1 ± 8.6 and 8.6 ± 9.0 m$^3$s$^{-1}$, respectively).

The temperature tended to increase from mid-spring (mean of 14.98 ± 2.33 °C) to mid-summer (mean 21.6 ± 1.66 °C) with a subsequent gradual decrease until winter (December, mean 11.6 ± 0.99 °C). The salinity showed values between 34.27 and 38.50. The highest salinities occurred from mid-summer to mid-autumn (July to October). The interannual variability of nitrates and silicates showed a similar seasonal pattern during the time series. Their

concentrations tended to increase from mid-autumn to winter (November to February), mean of 0.75 ± 1.22 and 2.04 ± 1.40 µmol L$^{-1}$ for nitrates, and 1.68 ± 1.46 and 2.13 ± 2.30 µmol L$^{-1}$, for silicates. Then, a decrease during summer was observed (0.11 ± 0.14 µmol L$^{-1}$ for nitrates and 1.12 ± 0.85 µmol L$^{-1}$ for silicates). Phosphate concentrations were low, with maxima in winter (average of 0.042 ± 0.043 µmol L$^{-1}$). Ammonium had two maxima, one in spring and one in autumn, reaching means of 0.30 ± 0.29 and 0.28 ± 0.22 µmol L$^{-1}$, respectively). Finally, chlorophyll a (Chl a) concentrations were higher in winter and had a mean value of 0.99 ± 0.83 µg L$^{-1}$.

## 3.2. Short term period (2012–2014)

### 3.2.1. Hydrological parameters

The temperature and salinity dynamics followed well-defined seasonal patterns (Fig. 2). Temperature values were lowest in February (9.4 and 12.7 °C for 2013 and 2014, respectively) and highest (24.0 °C) in August (Fig. 2a), while salinity ranged from 34.28 to 38.49 and showed two minima, the first in March 2013 and the second in January 2014. These minima (34.71 and 34.28, respectively) were exceptionally low (93% and 91% lower than the average for the last 14 years, respectively; Fig. 2b). On the other hand, the flow of the Têch and Têt Rivers showed high intra-seasonal variability. The maximum discharges of the two rivers in the study area occurred in early and mid-spring and corresponded to rainy periods (34.0 and 27.0 m$^3$s$^{-1}$ for the Têch River; 43.5 and 32.5 m$^3$s$^{-1}$ for the Têt River, Fig. 2c, d). During the dry periods the water flow decreased to 2 m$^3$s$^{-1}$.
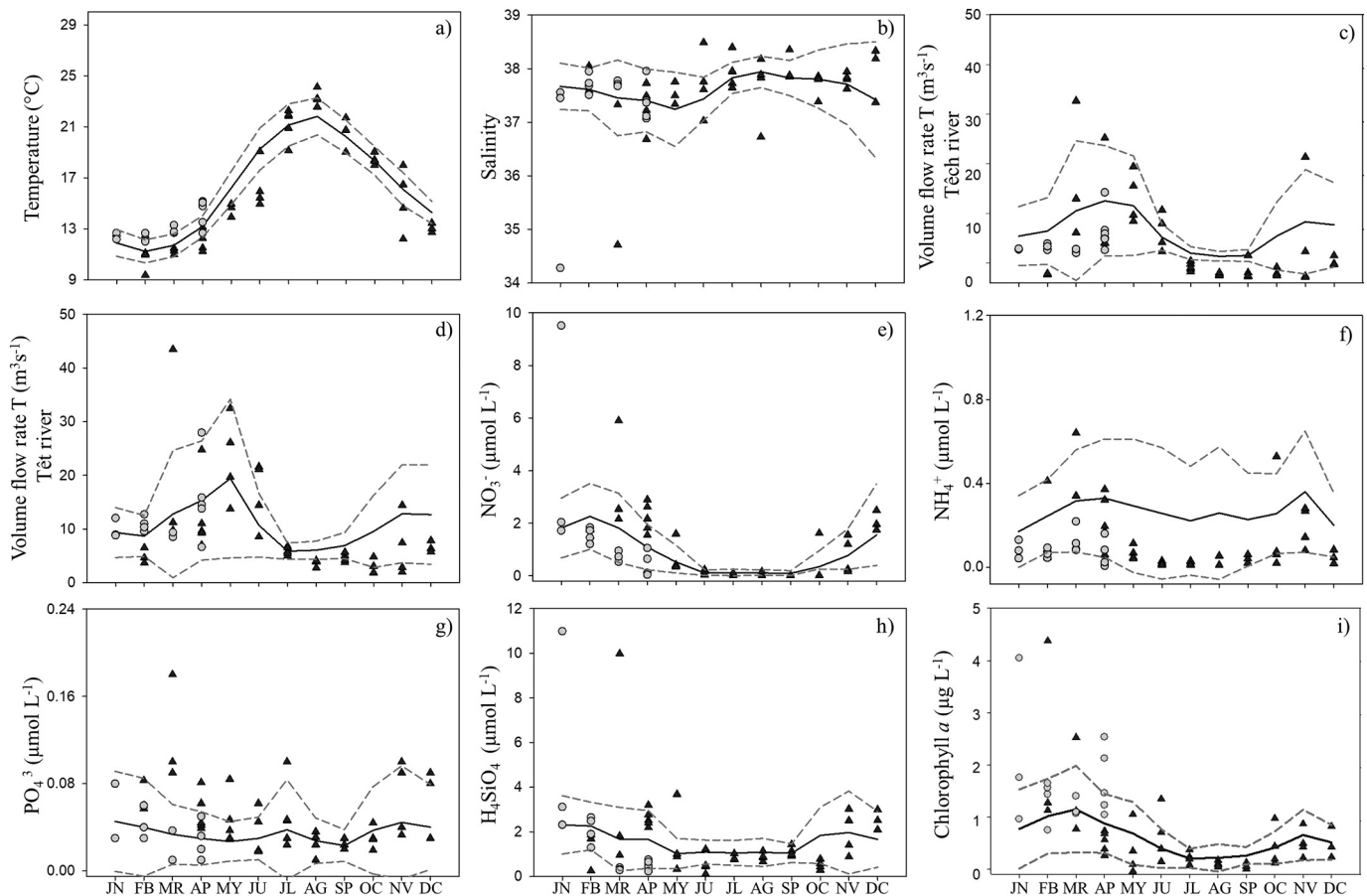


**Fig. 2.** Time series. a) Temperature (°C), b) salinity, c) discharge from the Têch River (m$^3$s$^{-1}$), d) discharge from the Têt River (m$^3$s$^{-1}$), (e–h) nitrate, ammonium, phosphate and silicate (µmol L$^{-1}$) and i) chlorophyll a (µg L$^{-1}$). The plots indicate the average annual cycle of each variable during 2000–2014; each month displays the average value (black line) ± standard deviation (dotted grey line) of that particular month. Triangles and circles represent 2013 and 2014 sampling respectively.
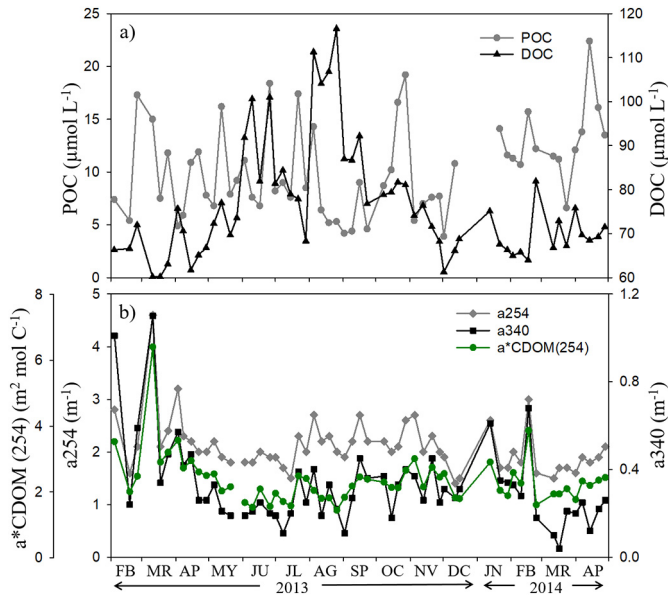
**Fig. 3.** Times series from February 2013 to April 2014. (a) Particulate and dissolved organic carbon (POC and DOC in µmol L$^{-1}$) and (b) absorption coefficient (a254 and a340, in m$^{-1}$ and specific absorption coefficient (a*CDOM(254), in m$^2$ mol C$^{-1}$).

### 3.2.2. Inorganic nutrients and chlorophyll a

Similarly, to the longer time series, inorganic nutrient concentrations were generally lower in summer than in winter and spring. Nitrate concentrations ranged from 0.02 µmol L$^{-1}$ to 9.5 µmol L$^{-1}$ (Fig. 2e), with values >5.0 µmol L$^{-1}$ in early-mid winter (March 2013 and January 2014). Ammonium concentrations ranged between 0.01 µmol L$^{-1}$ and 0.64 µmol L$^{-1}$ (Fig. 2f), showing remarkably low values in late spring and autumn 2013 (<0.1 µmol L$^{-1}$). The phosphate concentration was low (<0.2 µmol L$^{-1}$) throughout the entire time series (Fig. 2g). Silicate showed two maxima, one in March 2013 and one January 2014 (9.9 µmol L$^{-1}$ and 11 µmol L$^{-1}$ respectively, Fig. 2h), coinciding with the salinity minima (Fig. 2b) and with high nitrate values (Fig. 2e). Total chlorophyll (Chl *a*) ranged from 0.05 µg L$^{-1}$ to 4.39 µg L$^{-1}$ (Fig. 2i) and showed two peaks (February 2013 and January 2014) with concentrations of 4.39 µg L$^{-1}$ and

4 µg L$^{-1}$, respectively. The winter Chl *a* peak in 2013 followed a NH$_4^+$ maximum, while the 2014 peak came after a salinity minimum. In contrast, during spring and summer, Chl *a* was rather low, reaching values of <0.6 µg L$^{-1}$.

### 3.2.3. Dissolved and particulate organic carbon

The dissolved organic carbon (DOC) concentration ranged from 60.2 µmol L$^{-1}$ to 116.6 µmol L$^{-1}$. Maximum values occurred in mid to late summer (August–September), followed by a gradual decrease until the winter period, when DOC values remained low (60.2 to 81.9 µmol L$^{-1}$, Fig. 3a). Particulate organic carbon (POC) concentrations showed high variability throughout the whole period (from 3.9 to 22.4 µmol L$^{-1}$, Fig. 3a) with low concentrations (5.4 µmol L$^{-1}$) in early spring, autumn and winter 2013. In contrast, the highest POC values occurred in mid-autumn 2013 and mid-spring 2014 (19.2 and 22.4 µmol L$^{-1}$, respectively). DOC dynamics were significantly correlated to those of temperature, nitrates and Chl a (Table 1).

### 3.2.4. Chromophoric DOM

CDOM absorption coefficients at 254 nm (a254) and 340 nm (a340) showed high variability during the studied period, ranging from 1.6 to 4.6 m$^{-1}$ and from 0.04 m$^{-1}$ to 1.10 m$^{-1}$ respectively (Fig. 3b). Both a254 and a340 coefficients had maxima (4.6 m$^{-1}$ and 1.1 m$^{-1}$, respectively) in mid-winter (11 March, 2013), concomitant with low salinity (34.71) and low temperature (12 °C). In January 2014, and also coinciding with a minimum of salinity (34.28), high a254 and a340 values were also observed (2.6 and 0.6 m$^{-1}$, respectively). The coincidence between low salinity and high CDOM values was confirmed by significant negative correlations between salinity and a254 and a340. These indexes were also correlated (positively) with inorganic nutrients (Table 1).

The specific absorption coefficient at 254 nm, a*CDOM (254), oscillated between 1.43 and 6.4 m$^{-2}$g C$^{-1}$ and the highest values coincided with the salinity minima (Fig. 3b). This parameter also showed significant correlations with salinity (Table 1).

The spectral slopes S$_{250-500}$ and S$_{275-295}$ did not follow a regular pattern during the time series. The values fluctuated from 0.008 to 0.030 (S$_{250-500}$) and from 0.016 to 0.041 (S$_{275-295}$) (Table 2). For the (S$_{275-295}$) slope, which is a surrogate of low molecular weight substances, the highest values were found in summer coinciding with high DOC concentrations. Significant negative correlations were found between the S$_{275-295}$ values and inorganic nutrients (nitrates,

**Table 1**

Correlation coefficients between physical and chemical parameters from February 2013 to April 2014. Colored cells indicate significant correlations (dark = $p < 0.01$, and light = $p < 0.05$). Abbreviations: temperature (T, °C), salinity (S), nitrates (NO$_3^-$), phosphates (PO$_4^{-3}$), silicates (H$_4$SiO$_4$), ammonium (NH$_4^+$) in µmol L$^{-1}$, chlorophyll a (Chl a, µg L$^{-1}$), dissolved organic carbon (DOC, µmol L$^{-1}$), Irradiance (I, W m$^{-2}$), fluorescence DOM (Peak–M, Peak–C, Peak–T, in QSU), CDOM absorption coefficients (a254 and a340, in m$^{-1}$), specific absorption coefficient at 254 nm [a*CDOM(254) in m$^{-2}$g C$^{-1}$], fluorescence quantum yield at 340 ([ϕ (340)]) and spectral slope (S$_{275-295}$).

| | T | S | NO$_3^-$ | PO$_4^{-3}$ | H$_4$SiO$_4$ | NH$_4^+$ | Chl a | DOC | I | Peak-C | Peak-M | Peak-T | a254 | a340 | a*CDOM(254) | ϕ340 |
|---|---|---|---|---|---|---|---|---|---|---|---|---|---|---|---|---|
| S | 0.25 | | | | | | | | | | | | | | | |
| NO$_3^-$ | -0.85 | -0.34 | | | | | | | | | | | | | | |
| PO$_4^{-3}$ | -0.37 | -0.27 | 0.53 | | | | | | | | | | | | | |
| H$_4$SiO$_4$ | -0.33 | -0.42 | 0.54 | 0.54 | | | | | | | | | | | | |
| NH$_4^+$ | -0.57 | -0.18 | 0.64 | 0.36 | 0.28 | | | | | | | | | | | |
| Chl a | -0.69 | -0.35 | 0.58 | 0.19 | 0.05 | 0.29 | | | | | | | | | | |
| DOC | 0.74 | 0.13 | -0.69 | -0.33 | -0.34 | -0.46 | -0.47 | | | | | | | | | |
| I | 0.74 | 0.16 | -0.68 | -0.10 | -0.22 | -0.42 | -0.69 | 0.59 | | | | | | | | |
| Peak-C | -0.57 | -0.55 | 0.53 | 0.20 | 0.34 | 0.29 | 0.62 | -0.47 | -0.58 | | | | | | | |
| Peak-M | -0.61 | -0.56 | 0.57 | 0.27 | 0.36 | 0.32 | 0.64 | -0.52 | -0.58 | 0.97 | | | | | | |
| Peak-T | -0.38 | -0.44 | 0.35 | 0.10 | 0.18 | 0.21 | 0.52 | -0.36 | -0.43 | 0.78 | 0.81 | | | | | |
| a254 | -0.01 | -0.50 | 0.08 | 0.30 | 0.28 | 0.18 | 0.02 | 0.03 | 0.13 | 0.31 | 0.29 | 0.26 | | | | |
| a340 | -0.30 | -0.38 | 0.35 | 0.41 | 0.48 | 0.31 | 0.20 | -0.23 | -0.05 | 0.46 | 0.47 | 0.40 | 0.72 | | | |
| a*CDOM(254) | -0.44 | -0.48 | 0.48 | 0.44 | 0.42 | 0.43 | 0.29 | -0.58 | -0.24 | 0.52 | 0.54 | 0.41 | 0.80 | 0.71 | | |
| ϕ340 | -0.34 | -0.26 | 0.29 | -0.12 | -0.02 | 0.07 | 0.45 | -0.25 | -0.57 | 0.57 | 0.56 | 0.43 | -0.34 | -0.43 | -0.13 | |
| S$_{275-295}$ | 0.54 | 0.45 | -0.53 | -0.46 | -0.49 | -0.38 | -0.41 | 0.37 | 0.32 | -0.54 | -0.55 | -0.45 | -0.63 | -0.90 | -0.73 | 0.27 |

All data were log$_{10}$-transformed prior to the analyses.

**Table 2**
Seasonal average of the spectral slopes from 250 to 500 ($S_{250-500}$), from 275 to 295 ($S_{275-295}$), absorption coefficient (a254 and a340, in $m^{-1}$) and fluorescence quantum yield at 340 ([$\phi$ (340)]) during the time series.

| | Winter | | Spring | | Summer | | Autumn | |
|---|---|---|---|---|---|---|---|---|
| | Range | Average | Range | Average | Range | Average | Range | Average |
| $S_{250-500}$ | 0.008–0.025 | 0.016 | 0.011–0.030 | 0.019 | 0.013–0.030 | 0.017 | 0.014–0.020 | 0.017 |
| $S_{275-295}$ | 0.016–0.039 | 0.028 | 0.019–0.041 | 0.030 | 0.025–0.039 | 0.031 | 0.021–0.031 | 0.028 |
| $\phi$340 | 0.11–0.87 | 0.44 | 0.08–0.51 | 0.28 | 0.08–0.25 | 0.14 | 0.15–0.59 | 0.26 |
| a254 | 1.50–4.60 | 2.06 | 1.59–3.22 | 2.03 | 1.90–2.69 | 2.21 | 1.43–2.66 | 2.10 |
| a340 | 0.04–1.10 | 0.37 | 0.11–0.57 | 0.27 | 0.11–0.45 | 0.29 | 0.25–0.61 | 0.35 |

phosphate, silicate and ammonium) and Chl *a*, while these slopes values were positively related to DOC and solar irradiance (Table 1).

### 3.2.5. Fluorescent DOM

Fluorescent DOM excitation-emission matrices (EEMs) showed marked fluorescence peaks in the areas corresponding to the protein-like and humic-like substances. The EEMs showed a marked temporal variability, with noticeable changes in fluorescence signals associated with the two most contrasting environmental events: (1) the intrusion of low salinity (34.71) waters in winter (Fig. 4a) and (2) the high light exposure and stratification occurring in summer (Fig. 4b). Coincident with the freshwater inputs, clearly defined peaks in the humic-like areas could be identified in the EEMs (Fig. 4a). For further analyses, we selected the following single excitation/emission wavelength pairs (as in Coble, 1996): 340/440 nm (peak–C), 320/410 nm (Peak-M), 280/350 nm (peak–T).

In the humic-like area, the most intense peaks appeared on 11 March 2013 with values of 2.9 and 3.0 QSU for peak–C and peak–M respectively (Fig. 5a). The protein-like FDOM, peak–T, ranged from 0.18 to 3.65 QSU and followed temporal dynamics similar to those of the humic-like substances (Fig. 5a). We could detect variability in the relative concentration of protein-like FDOM with respect to humic-like FDOM: The highest value of the peak–T/peak–C ratio was detected in

March 2013 (Fig. 5b), while low peak–T/peak–C ratios were observed during the minimum salinity periods.

The three FDOM peaks showed significant positive correlations with nitrate and Chl *a* and negative correlations with DOC, temperature and salinity (Table 1). Solar irradiance was negatively correlated to humic-like FDOM peaks–C and M (Table 1). During the autumn-winter period, multiple regression analyses showed that both salinity and Chl *a* significantly affected ($p < 0.05$) the dynamics of the three FDOM peaks (Table 3), although the partial coefficients and significance were always higher for salinity.

The fluorescence quantum yield at 340 nm ($\Phi$340) ranged from 0.08 to 0.87 (Table 2). The highest values of $\Phi$340 ($>0.50$) were observed in winter and spring. This parameter was positively related to Chl *a* (Table 1) and negatively related to irradiance ($r = -0.57$, $p < 0.01$, $n = 52$, Fig. 6).

## 4. Discussion

### 4.1. Physical and chemical parameters

Our results show a well-marked seasonal variability of temperature, salinity and nutrients in our study area, as previously described by other authors (Marty et al., 2002; Grémare et al., 2003). Two sharp decreases
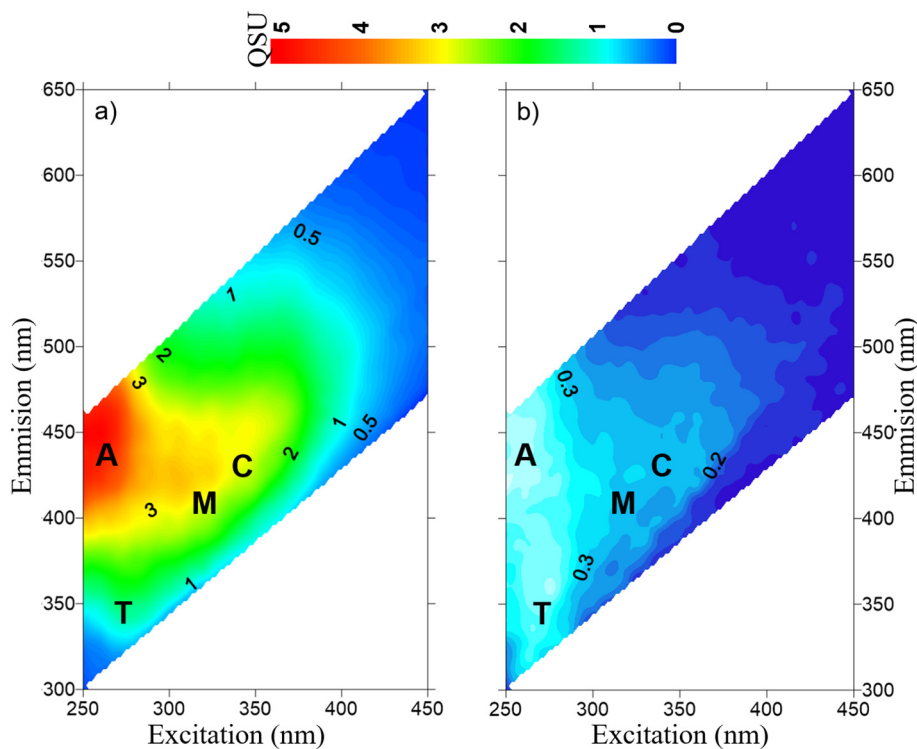


**Fig. 4.** Example EEMs showing the two most contrasting environmental events: a) intrusion of water with low salinity in winter and b) water photobleached in summer. Inside the EEMs, the capital letters indicate the different peaks: humic-like substances (Peak–A), terrestrial humic-like substances (Peak–C), marine humic-like substances (Peak–M) and protein-like substances (Peak–T).
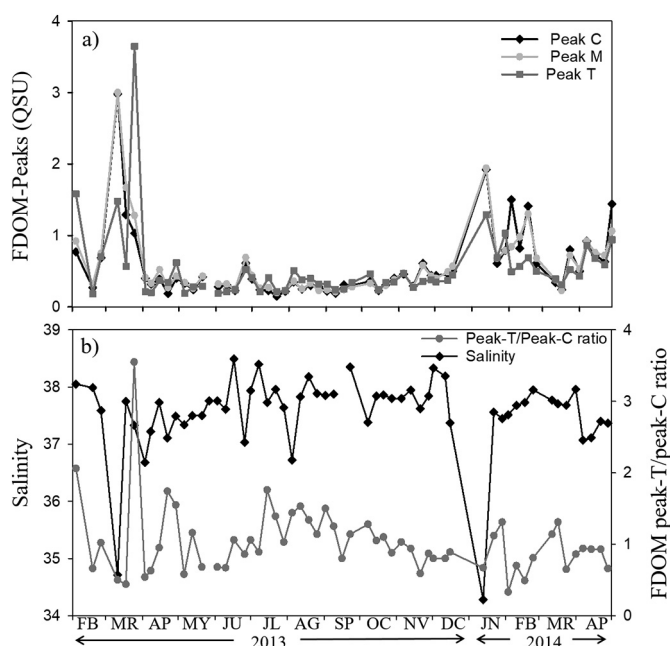
**Fig. 5.** Times series from February 2013 to April 2014. a) Fluorescent DOM (Peak–C and M humic-like FDOM, Peak–T protein-like FDOM). Fluorescence is expressed in quinine sulfate units (QSU) and b) Ratio between Peak–T and Peak–C, and salinity.



**Fig. 6.** Relationship between irradiance (W m$^{-2}$) and fluorescence quantum yield at 340 nm, [Φ (340)]. The lineal regression (black line) was calculated including all the data from the time series; Y = 0.67 (−0.00048)-4 X; $R^2$ = 0.358; $p$ < 0.01; $n$ = 52.

in salinity were observed in winter (11 March, 2013 and 13 January, 2014). Coinciding with the salinity minimum of March 2013, we observed high water discharges from the Têt and Têch Rivers (≈40 m$^3$s$^{-1}$ each). The salinity minimum in January 2014 could be associated with other environmental factors, such as rain or wind, since previous studies have noted their influence (e.g. NE tramontane winds) on the coastal ocean circulation (Estournel et al., 2005; Aparicio et al., 2017). Unfortunately, we do not have enough data to assess the relative contribution of hydrological factors other than river discharge; however, high nitrate and silicate concentrations were found during the salinity minima, which was confirmed by significant correlations ($r$ = −0.34 and −0.42; $p$ < 0.05, $n$ = 57). This could indicate that river flow was actually influencing the nutrient levels, and, for the case of January 2014, probably inducing a peak in chlorophyll $a$ (Fig. 2). The other Chl $a$ maximum was observed in February 2013. This peak did not follow any salinity minima but coincided with a relative maximum of NH$_4^+$. This ammonium peak could be originated by sediment resuspension caused by the strong wind observed during that period (mean 19 m s$^{-1}$, data not shown). High waves and swell have been reported as a cause for sediment resuspension at the SOLA station (Guizien et al., 2007). In fact, coinciding with this Chl $a$ peak, we found a relative minimum of temperature (Fig. 2) that could be a sign of water intrusion from deeper layers.

**Table 3**
Results of multiple regression analysis between FDOM peaks C, M, and T (log$_{10}$ R.U., dependent variables) and chlorophyll $a$ (Chl $a$) and salinity (log$_{10}$, independent variables) during the autumn-winter period in the SOLA station. $n$ = 26, b = non-standardized partial coefficient; β = standardized partial coefficient; $p$: level of significance.

| Dependent variable | Independent variables | | | | | | |
|---|---|---|---|---|---|---|---|
| | Salinity | | | Chl $a$ | | | |
| | b | β | $p$ | b | β | $p$ | $R^2$ |
| Peak-C | −13.9 | −0.529 | 0.002 | 0.273 | 0.345 | 0.034 | 0.537 |
| Peak-M | −13.0 | −0.492 | 0.004 | 0.300 | 0.377 | 0.023 | 0.524 |
| Peak-T | −10.0 | −0.470 | 0.006 | 0.252 | 0.391 | 0.020 | 0.513 |
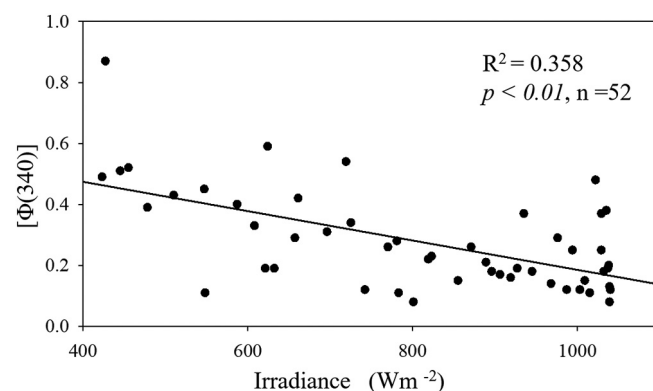
We compared the results obtained for the 2012–2014 period with climatological and environmental data collected from 2000 to 2014 at the same station. We found that the values for the different variables during the 2012–2014 period, in general, varied within the range of the values observed in the past 14 years. There were, however, two salinity outliers. The annual salinity minima found in our study were also the minima for the last 14 years. Considering that these minima are associated with extremely high nutrient concentrations, it would be of interest to check whether these phenomena are sporadic or, conversely, associated with a shift in meteorological trends. Notably, the ammonia concentration values were, in general, below the mean of the past 14 years, while the phosphate values tended to be above the average. This change in the tendency in nutrient dynamics may be due to local processes because it did not occur in other coastal areas of the NW Mediterranean close to the SOLA study site (e.g. the Blanes Bay Microbial Observatory, Nunes et al., 2018).

### 4.2. Temporal mismatch between dissolved organic matter and inorganic nutrients

In our study site and period, we observed an accumulation of dissolved organic carbon (DOC) towards the end of summer, also observed in previous studies in the NW Mediterranean Sea (Copin-Montégut and Avril, 1993; Vila-Reixach et al., 2012; Romera-Castillo et al., 2013) and in other oligotrophic ocean areas (Carlson and Hansell, 2015). This accumulation in summer has been attributed to the "malfunctioning of the microbial loop" (Thingstad et al., 1997); that is, the inability of heterotrophic prokaryotes to uptake DOM due to the limitation in inorganic nutrients. Although the Mediterranean Sea is mainly limited by phosphorus, and subsequent studies have also proven this limitation in the NW area (Sala et al., 2002; Salter et al., 2014; Pinhassi et al., 2006), the concentrations of both dissolved nitrogen and phosphorus are extremely low in summer (close to detection limits 0.05 and 0.02 μmol L$^{-1}$, respectively), and osmotrophs are probably limited by both nutrients as Sala et al. (2002) also pointed out. Nevertheless, in other NW Mediterranean zones, relatively high heterotrophic prokaryotic production, measured as leucine incorporation, has been found in summer, coinciding with the lowest inorganic nutrient concentrations (Alonso-Sáez et al., 2008; Laghdass et al., 2010). Later, Vila-Reixach et al. (2012) proposed that accumulated DOC comes from heterotrophic prokaryotic origin. To interpret this mismatch between DOC accumulation and heterotrophic prokaryotic activity, more detailed studies need to be carried out. Top-down control could also contribute to this mismatch, as grazing is also a significant DOM source (Strom et al., 1997). In fact, several studies have reported increases in grazing activity with temperature (Marrasé et al., 1992; Vaqué et al., 1994; Unrein et al., 2007).

*4.3. Seasonal dynamics of CDOM fractions*

At SOLA station we could observe that the sharpest changes in the quality of the FDOM coincided with high river discharges. In fact, the significant negative correlations between FDOM peaks and salinity suggest that the incoming fresh waters have a high FDOM content (Table 1) in line with previous studies showing that CDOM and FDOM concentrations in coastal areas are influenced by terrestrial-derived inputs (Ferrari, 2000; Blough and Del Vecchio, 2002). However, based on our results we hypothesize that, during most of the year, the variability in humic-like FDOM in the coastal Mediterranean Sea depends on a combination of biotic and abiotic factors, and that the autochthonous DOM inputs (e.g. exudation from marine phytoplankton or heterotrophic prokaryotes) (Alonso-Sáez et al., 2009; Romera-Castillo et al., 2011a; Kramer and Herndl, 2004; Jørgensen et al., 2014) are the main source and photobleaching after sunlight exposure is the main sink (see below).

The significant correlations between all FDOM peaks and chlorophyll could be indicative of a phytoplanktonic source. This contrasts with the lack of correlation between Chl *a* and DOC and with the negative correlation between DOC and the humic-like FDOM peaks (Table 1). This reflects that the autochthonous processes controlling these two pools of organic matter are uncoupled and are affecting their dynamics in opposite directions (Chen and Bada, 1992; Coble, 2007; Romera-Castillo et al., 2013). On the one hand, phytoplankton have been shown to produce humic-like and protein-like FDOM (Romera-Castillo et al., 2010), which could be manifested in our study systems in winter and autumn, when other sources and the main sinks (i.e. photobleaching, see below) are minor. In fact, multiple regression analysis performed with winter and autumn FDOM data for the humic-like peaks (C and M) and also for the protein-like peak (T) revealed significant relationships with both salinity and Chl *a* (see Table 3). This corroborates that, although land inputs highly influence the FDOM dynamics, in situ biological activity may also contribute to this variability. On the other hand, the increase in FDOM peaks associated with increases in phytoplankton biomass could be also indirect and mediated by bacterial reprocessing (Coble et al., 1998; Romera-Castillo et al., 2011b).

Low concentrations of humic-like FDOM found during the stratification period (April to October) coincided with high sunlight exposure (on average: day length 14 h d$^{-1}$, irradiance 903 W m$^{-2}$). Thus, photobleaching could be the major FDOM sink during this period. Similar trends have been observed in other coastal areas (Para et al., 2010; Romera-Castillo et al., 2013), where humic-like compounds were also low in summer. This pattern was paralleled by the highest values of $S_{275-295}$ (Table 2) found in summer, when DOC concentrations were also elevated. High $S_{275-295}$ values indicate low molecular weight (LMW) material, possibly photobleaching products (Helms et al., 2008), and, indeed, we observed negative correlations between Irradiance and $S_{275-295}$ (Table 1). According to the Size-Reactivity Continuum hypothesis (Benner and Amon, 2015) most of the refractory DOC resides in LMW molecules, and thus increased photobleaching in summer would increase the refractory, i.e. resistant to biodegradation, DOC fraction (Obernosterer et al., 1999), favoring the observed accumulation of DOC in summer. Finally, decreases in fluorescence quantum yield at 340 nm, [Φ (340)], are also related to photobleaching (Romera-Castillo et al., 2011b, 2013). We found a significant negative relationship between [Φ (340)] and Irradiance (Fig. 6), which corroborates with photobleaching being a main driver of humic-like FDOM decreases in summer.

## 5. Conclusions

The seasonal patterns of the environmental variables studied could be discerned clearly. The signal of episodic events, such as fresh water intrusions, on DOM dynamics could be captured thanks to the high sampling frequency. During the study period, we found a temporal mismatch between autotrophic biomass (chlorophyll *a*) and dissolved organic carbon, although correlations between chlorophyll *a* and FDOM peaks suggest an autochthonous DOM source that drives their dynamics during most of the year and, in particular, in winter-autumn seasons. In summer, when the water column was highly stratified, we observed the highest DOC concentrations concomitant with the lowest chlorophyll *a* values. Yet, the high DOC concentration in summer coincided with low fluorescence intensities of the humic-like DOM fractions. We attributed this temporal decoupling to photobleaching processes, which are also indicated by lower fluorescence quantum yields. We propose that photobleaching is one of the main mechanisms rendering DOC recalcitrant, so that it accumulates in the water column during summer. We postulate that a combination of episodic terrestrial inputs, photobleaching in summer, and microbial activity, could subsequently explain the different DOC dynamics and its optically active fractions.

## References

Alonso-Sáez, L., Vázquez-Domínguez, E., Cardelús, C., Pinhassi, J., Sala, M.M., Lekunberri, I., Gasol, J.M., 2008. Factors controlling the year-round variability in carbon flux through bacteria in a coastal marine system. Ecosys 11, 397–409.

Alonso-Sáez, L., Unanue, M., Latatu, A., Azua, I., Ayo, B., Artolozaga, I., Iriberri, J., 2009. Changes in marine prokaryotic community induced by varying types pf dissoved organic matter and subsequent grazing pressure. Plankton Res 31, 1373–1383.

Aparicio, F.L., Nieto-Cid, M., Calvo, E., Pelejero, C., Lopez-Sanz, A., Pascual, J., Salat, J., Sánchez-Pérez, E.D., Gasol, J.M., Marrasé, C., 2017. Wind- induced changes in the dynamics of fluorescent organic matter in the coastal NW Mediterranean. Sci. Total Environ. 609, 1001–1012.

Benner, R., Amon, R.M., 2015. The size-reactivity continuum of major bioelements in the ocean. Annu. Rev. Mar. Sci. 7, 185–205.

Blough, N.V., Del Vecchio, R., 2002. Chromophoric DOM in the coastal environment. In: Hansell, D.A., Carlson, C.A. (Eds.), Biogeochemistry of Marine Dissolved Organic Matter. Academic Press, San Diego, pp. 509–540.

Böhm, E., Riminucci, F., Bortoluzzi, G., Colella, S., Acri, F., Santoleri, R., Ravaioli, M., 2016. Operational use of continuous surface fluorescence measurements offshore Rimini to validate satellite-derived chlorophyll observations. Oper. Oceanogr. 9, 167–175.

Bricaud, A., Morel, A., Prieur, L., 1981. Absorption by dissolved organic-matter of the sea (yellow substance) in the UV and visible domains. Limnol. Oceanogr. 26, 43–53.

9

Carlson, C.A., Hansell, D.A., 2015. DOM sources, sinks, reactivity and budgets. In: Hansell, D.A., Carlson, C.A. (Eds.), Biogeochemistry of Marine Dissolved Organic Matter, 2nd ed Academic Press, pp. 65–126. https://doi.org/10.1016/B978-0-12-405940-5.00003-0.

Cauwet, G., 1999. HTCO method for dissolved organic carbon analysis in seawater: influence of catalyst on blank estimation. Mar. Chem. 47, 55–64.

Chen, R.F., Bada, J.L., 1992. The fluorescence of dissolved organic matter in seawater. Mar. Chem. 37, 191–221. https://doi.org/10.1016/0304-4203(92)90078-O.

Cloern, J.E., Jassby, A., 2008. Complex seasonal patterns of primary producers at the land-sea interface. Ecol. Lett. 11, 1249–1303.

Coble, P.G., 1996. Characterization of marine and terrestrial DOM in seawater using excitation-emission matrix spectroscopy. Mar. Chem. 51, 325–346. https://doi.org/10.1016/0304-4203(95)00062-3.

Coble, P.G., 2007. Marine optical biogeochemistry: the chemistry of ocean color. Chem. Rev. 107, 402–418. https://doi.org/10.1021/cr0503501.

Coble, P.G., Del Castillo, C.E., Avril, B., 1998. Distribution and optical properties of CDOM in the Arabian Sea during the 1995 Southwest Monsoon. Deep-Sea. Res. PT II. 45, 2195–2223. https://doi.org/10.1016/S0967-0645(98)00068-X.

Copin-Montégut, G., Avril, B., 1993. Vertical distribution and temporal variation of dissolved organic carbon in the North-Western Mediterranean Sea. Deep-Sea. Res. PT I. 40 (10), 1963–1972.

De La Fuente, P., Marrasé, C., Canepa, A., Álvarez-Salgado, X.A., Gasser, M., Fajar, N.M., Romera-Castillo, C., Pelegrí, J.L., 2014. Does a general relationship exist between fluorescent dissolved organic matter and microbial respiration? The case of the dark equatorial Atlantic Ocean. Deep-Sea Res. PT I. 89, 44–55. https://doi.org/10.1016/j.dsr.2014.03.007.

Estournel, C., Durrieu de Madron, X., Marsaleix, P., Auclais, P., Julliand, C., Vehil, R., 2005. Observation and modeling of the winter coastal oceanic circulation in the Gulf of Lion under wind conditions influenced by the continental orography (FETCH experiment). J. Geophys. Res. 108, 8059.

Ferrari, G., 2000. The relationship between chromophoric dissolved organic matter and dissolved organic carbon in the European Atlantic coastal area and in the West Mediterranean Sea (Gulf of Lions). Mar. Chem. 70, 339–357.

Green, S.A., Blough, N.V., 1994. Natural waters optical absorption and fluorescence of chromophoric properties dissolved organic matter in natural waters. Limnol. Oceanogr. 39 (8), 1903–1916.

Grémare, A., Amouroux, J.M., Cauwet, G., Charles, F., Courties, C., De Bovée, F., Dinet, A., Devenon, J.L., Durrieu De Madron, X., Ferre, B., Fraunie, P., Joux, F., Lantoine, F., Lebaron, P., Naudin, J.J., Albert, Palanques, Pujo-Pay, M., Zudaire, L., 2003. The effects of a strong winter storm on physical and biological variables at a shelf site in the Mediterranean. Oceanology Acta 26 (4), 407–419.

Guizien, K., Charles, F., Lantoine, F., Naudin, J.J., 2007. Nearshore dynamics of nutrients and chlorophyll during Mediterranean-type flash floods. Aquat. Living Resour. 20 (1), 3–14.

Hancke, K., Hovland, E.K., Volent, Z., Pettersen, R., Johnsen, G., Moline, M., Sakshaug, E., 2014. Optical properties of CDOM across the polar front in the Barents Sea: origin, distribution and significance. J. Mar. Syst. 130, 219–227.

Hedges, J.I., 2002. Why dissolved organics matter. In: Hansell, D.A., Carlson, C.A. (Eds.), Biogeochemistry of Marine Dissolved Organic Matter. Academic Press, Oxford.

Helms, J.R., Stubbins, A., Ritchie, J.D., Minor, E.C., David, J., Mopper, K., Kieber, D.J., 2008. Absorption spectral slopes and slope ratio as indicators of molecular source, slopes and slope ratios absorption spectral of chromophoric and photobleaching dissolved matter organic. Limnol. Oceanogr. 53 (3), 955–969.

Holmes, M.R., Aminot, A., Kérouel, R., Hooker, B.A., Peterson, B.J., 1999. A simple and precise method for measuring ammonium in marine and freshwater ecosystems. Journal Fish Aquat. Sci. 56, 1801–1808.

Holm-Hansen, O., Lorenzen, C.J., Holmes, R.W., Strickland, J.D.H., 1965. Fluorimetric determination of chlorophyll. Mar. Sci. 30, 3–15.

Jørgensen, L., Stedmon, C.A., Granskog, M.A., Middelboe, M., 2014. Tracing the long-term microbial production of recalcitrant fluorescent dissolved organic matter in seawater. Geophys. Res. Lett. 41, 2481–2488. https://doi.org/10.1002/2014GL059428.

Kothawala, D.N., Murphy, K.R., Stedmon, C.A., Weyhenmeyer, G.A., Tranvik, L.J., 2013. Inner filter correction of dissolved organic matter fluorescence. Limnol. Oceanogr. Meth. 11, 616–630.

Kramer, G.D., Herndl, G.J., 2004. Photo and bioreactivity of chromophoric dissolved organic matter produced by marine bacterioplankton. Aquat. Microb. Ecol. 36, 239–246.

Kuwahara, V.S., Ogawa, H., Toda, T., Kilkuchi, T., Taguchi, S., 2000. Variability of bio-optical factors influencing the seasonal attenuation of ultraviolet radiation in temperate coastal waters of Japan. Photochem. Photobiol. 72, 193–199.

Laghdass, M., West, N.J., Batailler, N., Caoarros, J., Catala, P., Lantoine, F., Oriol, L., Lebaron, P., Obesnosterer, I., 2010. Impact of lower salinity waters on bacterial heterotrophic production and community structure in the offshore NW Mediterranean Sea. Environ. Microbiol. Rep. 2 (6), 761–769.

Marrasé, C., Lim, E.L., Caron, D.A., 1992. Seasonal and daily changes in bacterivory in a coastal plankton community. Mar. Ecol. Progr. Ser. 82, 281–289.

Marty, J.C., Chiavérine, J., Pizay, M.D., Bernard, A., 2002. Seasonal and interannual dynamics of nutrients and phytoplankton pigments in the western Mediterranean Sea at the DYFAMED time-series station (1991–1999). Deep-Sea Res. PT II. 49, 1965–1985.

Melhuish, W.H., 1961. Quantum efficiencies of fluorescence of organic substances: effect of solvent and concentration of the fluorescent solute. J. Phys. Chem. 65, 229–235.

Nelson, N.B., Craig, A.C., Steinberg, D.K., 2004. Production of chromophoric dissolved organic matter by Sargasso Sea microbes. Mar. Chem. 89, 273–287.

Nieto-Cid, M., Álvarez-Salgado, X.A., Pérez, F.F., 2006. Microbial and photochemical reactivity of fluorescent dissolved organic matter in a coastal upwelling system. Limnol. Oceanogr. 51, 1391–1400.

Nunes, S., Latasa, M., Gasol, J.M., Estrada, M., 2018. Seasonal and interannual variability of phytoplankton community structure in a Mediterranean coastal site. Mar. Ecol. Progr. Ser. 592, 57–75.

Obernosterer, I., Reitner, B., Herndl, G.J., 1999. Contrasting effects of solar radiation on dissolved organic matter and its bioavailability to marine bacterioplankton. Limnol. Oceanogr. 44, 1645–1654.

Ohno, T., 2002. Fluorescence inner-filtering correction for determining the humification index of dissolved organic matter. Environ. Sci. Technol. 36, 742–746.

Para, J., Coble, P.G., Charrière, B., Tedetti, M., Fontana, C., Sempéré, R., 2010. Fluorescence and absorption properties of chromophoric dissolved organic matter (CDOM) in coastal surface waters of the northwestern Mediterranean Sea influence of the Rhône River. Biogeosci. Discuss. 7, 4083–4103.

Pinhassi, J., Gomez-Consarnau, L., Alonso-Saez, L., Sala, M.M., Vidal, M., Pedros-Alio, C., Gasol, J.M., 2006. Seasonal changes in bacterioplankton nutrient limitation and their effects on bacterial community composition in the NW Mediterranean Sea. Aquatic Microbiol. Ecol. 44, 241–252.

Pujo-Pay, M., Raimbault, P., 1994. Improvement of the wet-oxidation procedure for simultaneous determination of particulate organic nitrogen and phosphorus collected on filters. Marine Ecol. Progr. Ser. 105, 203–207.

Romera-Castillo, C., Sarmento, H., Álvarez-Salgado, X.A., Gasol, J.P., Marrasé, C., 2010. Production of chromophoric dissolved organic matter by marine phytoplankton. Limnol. Oceanogr. 55 (1), 446–454. https://doi.org/10.4319/lo.2010.55.1.0446.

Romera-Castillo, C., Nieto-Cid, M., Castro, C.C., Marrasé, C., Largier, J., 2011a. Fluorescence: absorption coefficient ratio — tracing photochemical and microbial degradation processes affecting coloured dissolved organic matter in a coastal system. Mar. Chem. 125, 26–38. https://doi.org/10.1128/AEM.00200-11.

Romera-Castillo, C., Sarmento, H., Álvarez-Salgado, X.A., Gasol, J.M., Marrasé, C., 2011b. Net production/consumption of fluorescent coloured dissolved organic matter by natural bacterial assemblages growing on marine phytoplankton exudates. Appl. Environ. Microbiol. 77, 7490–7498.

Romera-Castillo, C., Álvarez-Salgado, X.A., Galí, M., Gasol, J.M., Marassé, C., 2013. Combined effect of light exposure and microbial activity on distinct dissolved organic matter pools. A seasonal field study in an oligotrophic coastal system (Blanes Bay, NW Mediterranean). Mar. Chem. 148, 44–51.

Romero, E., Peters, F., Arin, L., Guillén, J., 2014. Decreased seasonality and high variability of coastal plankton dynamics in an urban location of the NW Mediterranean. J. Sea Res. 88, 130–143.

Sala, M.M., Peters, F., Gasol, J.M., Pedrós-Alió, C., Marrasé, C., Vaqué, D., 2002. Seasonal and spatial variations in the nutrient limitation of bacterioplankton growth in the north-western Mediterranean. Aquat. Microbiol. Ecol. 27 (1), 47–56.

Salter, I., Galand, P.E., Catala, P., Courties, C., Fagervold, S.K., Lebaron, P., Obernosterer, I., Oliver, M.J., Suzuki, M.T., Tricoire, C., 2014. Dynamics of inorganic and organic phosphorous substrate utilization by extant microbial populations in the North-West Mediterranean Sea. 2014 Ocean Sciences Meeting 2014, Honolulu, Hawaii, USA, 23 February 2014–28 February 2014.

Stedmon, C.A., Bro, R., 2008. Characterizing dissolved organic matter fluorescence with parallel factor analysis: a tutorial. Limnol. Oceanograph-Meth. 6, 572–579.

Strom, S.L., Benner, R., Ziegler, S., Dagg, M.J., 1997. Planktonic grazers are a potentially important source of marine dissolved organic carbon. Limnol. Oceanogr. 42, 1364–1374.

Sugimura, Y., Suzuki, Y., 1998. A high temperature catalytic oxydation method for the determination of non-volatile dissolved organic carbon in sea water by direct injection of a liquid sample. Mar. Chem. 24, 105–131.

Thingstad, T.F., Hagstrom, A., Rassoulzadegan, F., 1997. Accumulation of degradable DOC in surface waters: is it cause by a malfunctioning microbial loop? Limnol. Oceanogr. 42 (2), 398–404.

Unrein, F., Massana, R., Alonso-Sáez, L., Gasol, J.M., 2007. Significant year-round effect of small mixotrophic flagellates on bacterioplankton in an oligotrophic coastal system. Limnol. Oceanogr. 52 (1), 456–469.

Vaqué, D., Gasol, J.M., Marrasé, C., 1994. Grazing rates on bacteria: the significance of methodology and ecological factors. Mar. Ecol. Progr. Ser. 109, 263–274.

Vila-Reixach, G., Gasol, J.M., Cardelús, C., Vidal, M., 2012. Seasonal dynamics and net production of dissolved organic carbon in an oligotrophic coastal environment. Mar. Ecol. Prog. Ser. 456, 7–19.

Wagner, S., Schubotz, F., Kaiser, K., Hallmann, C., Waska, H., Rossel, P.E., Hansman, R., Elvert, M., Middelburg, J.J., Engel, A., Blattmann, T.M., Catalá, T.S., Lennartz, S.T., Gomez-Saez, G.V., Pantoja-Gutiérrez, S., Bao, R., Galy, V., 2020. Soothsaying DOM: a current perspective on the future of oceanic dissolved organic carbon. Front. Mar. Sc. https://doi.org/10.3389/fmars.2020.00341.

Wang, T., Zeng, L.H., Li, D.L., 2017. A review on the methods for correcting the fluorescence inner-filter effect of fluorescence spectrum. Appl. Spectrosc. Rev. 52, 883–908.

Weishaar, J.L., Aiken, G.R., Bergamaschi, B.A., Fram, M.S., Fujii, R., Mopper, K., 2013. Evaluation of specific ultraviolet absorbance as an indicator of the chemical composition and reactivity of dissolved organic carbon. Environ. Sci. Technol 37, 4702–4708.

Yamashita, Y., Tanoue, E., 2003. Chemical characterization of protein-like fluorophores in DOM in relation to aromatic amino acids. Mar. Chem. 82, 255–271. https://doi.org/10.1016/S0304-4203(03)00073-2.